Electronic Supplementary Information:

A Comprehensive Optical Analysis of Nanoscale Structures: from Thin Films to Asymmetric Nano-cavities

Giuseppe Emanuele Lio, Giovanna Palermo, Roberto Caputo, and

Antonio De Luca*

CNR-Nanotec, Consiglio Nazionale della Ricerca, sede di Cosenza and Dipartimento di Fisica,

Università della Calabria, 87036 Arcavacata di Rende (CS), Italy

E-mail: antonio.deluca@fis.unical.it

Geometry, mesh and local variables

The proposed numerical ellipsometric analysis has been performed by using the COMSOL Multiphysics platform, that gives the possibility to use a 2D or 3D environment. The 3D geometry built in COMSOL is composed by a parallelepiped with a height of $3 \cdot d$, where d is the edge length which is typically comparable with the minimum wavelength value, in our case this is set to $\lambda = 400nm$. The choice of d is fundamental for the optimal propagation of the lightwave inside the system preventing any diffraction or boundary problems. The numerical setup of the NEA model is sketched in Fig. S1a, with the three blocks representing the superstrate (air), the substrate (glass) and the multi-layer system well in evidence. In COMSOL sources or detectors of electromagnetic radiation are created by using ports by which the radiation enters or exits the

1

simulated system. In our case, there is a port (Port$_{in}$) on the top from where the radiation is emitted and a port on the bottom (Port$_{out}$) that behaves as a detector. There are several kinds of ports, user defined, periodic, rectangular, circular depending on the particular requirement of the physical problem. In order to model our system in the correct way, the xy plane is considered infinite. This choice can be reproduced in COMSOL by using periodic ports. In our model, a periodic port (representing the source) is placed on the top of the parallelepiped and it is configured as "active port". A second port is placed on the bottom of our geometry, representing the detector, and it is configured as "active-off port". Then, periodic boundary conditions (PBCs) are applied to the four faces of the geometry, along x and y directions (Fig. S1b) paired two-by-two. The PBCs ensure the above mentioned infinite conditions. An important role in the numerical system is carried out by the mesh that discretizes the problem. COMSOL Multiphysics gives the opportunity to set it as controlled by the physics, by selecting the option "physics-controlled the mesh" present in "physics study". A "normal mesh" is automatically generated by the software, depending on the minimal size present in the system, compared with the incident wavelength (Fig. S1c). To analyze simultaneously TE and TM polarized waves, the user has to add two "physics", belonging to the "Electromagnetic Waves, Frequency Domain" module (identified in the software as "emw"). The two distinct "physics" are used to evaluate the two reflectances R_p and R_s simultaneously, necessary to calculate the ellipsometric angles Ψ and Δ.
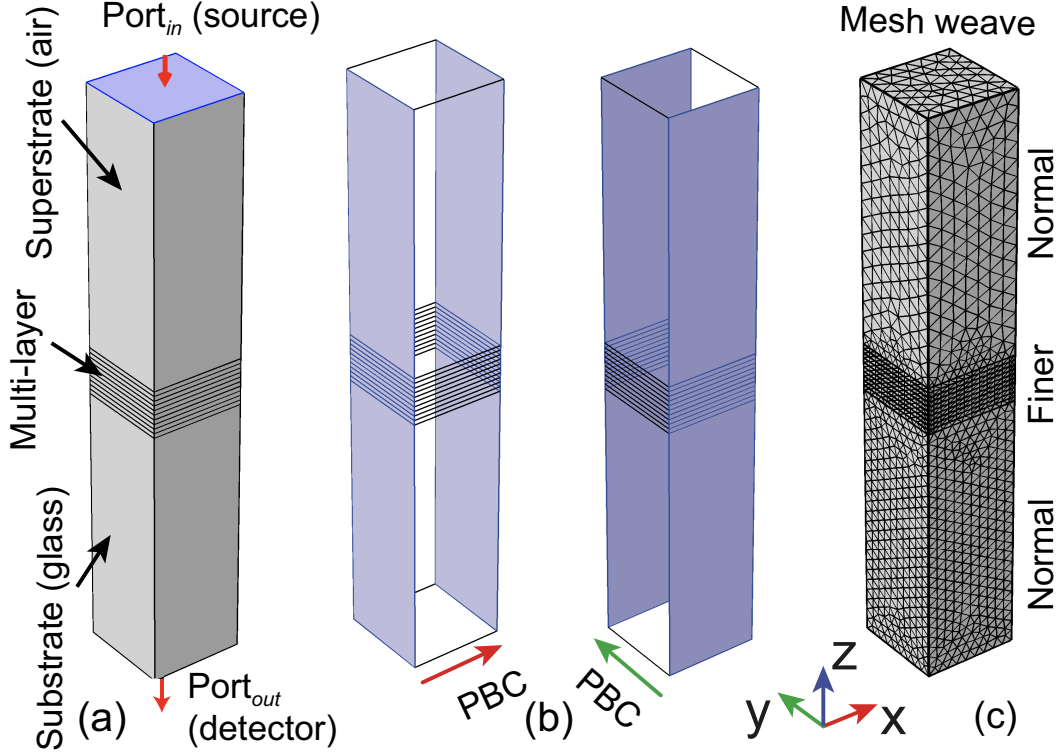
Figure S1: (a) The main structure of the NEA model, it is realized from a parallelepiped divided in layers that constitute the superstrate, the layer of materials and the substrate. (b) Here it is shown the application direction of the periodic boundary condition from periodic port. (c) A sketch of the mesh directly controlled from the physics, the larger part are meshed with a normal weave while for the small parts has been used a fine mesh weave.

We recall that ρ is defined as $\rho = \widetilde{r}_p/\widetilde{r}_s$; $\widetilde{r}_p$ and $\widetilde{r}_s$ are the complex Fresnel coefficients. Then, being $\rho = \tan(\Psi)e^{i\Delta}$, $\Psi = (arctan(r_p/r_s))$, where $r_{p,s}$ represent the real parts of the Fresnel coefficients ($r_{p,s} = \sqrt{R_{p,s}}$), while Δ is related to the imaginary part of ρ, $\Delta = [\Im(\ln r_p/r_s) + \pi]$. To obtain quantities comparable to the experimental curves, the variables have to be multiplied by $180/\pi$ to convert them from radians to degrees.

Dispersion relations and cavity modes in 2- and 3-BMM

The N-BMMs present a peculiar optical behavior by selectively transmitting light in the UV-VIS-NIR spectrum. This particular feature is achieved without using diffraction gratings or other super-structures to couple in the impinging wavevector. The presence of optical modes within the cavities

can be explained by considering the dispersion relation of gap surface plasmons (gsp) and channeling plasmon polaritons (cpp). By using a Matlab code, it is possible to evaluate the dispersion relation (DR)[1,2] of the two realized structures. In case of a metal/insulator/metal (MIM) structure, the dispersion relation involving the wave vector β can be written as:

$$tanh\left[\frac{\alpha_d t_{cav}}{2}\right] = -\frac{\varepsilon_d \alpha_m}{\varepsilon_m \alpha_d} \tag{1}$$

Here $\varepsilon_{m,d}$ are the dielectric constants of the metal and dielectric materials, respectively whereas t_{cav} is the thickness of the insulator cavity and $\alpha_{m,d} = \sqrt{\beta_{gsp}^2 - \varepsilon_{m,d}k_0^2}$. By solving the dispersion relation with the approximation $tanh(x) \approx 1 - 2e^{2x}$, it is possible to find the following expression for β_{gsp}[3–5]:

$$\beta_{gsp} = \beta_{spp}\sqrt{1 - \frac{4\varepsilon_d\varepsilon_m}{\varepsilon_m^2 - \varepsilon_d^2}exp(-\alpha_1 t_{cav})} \tag{2}$$

with

$$\alpha_1 = \alpha_0\sqrt{1 + \frac{4\varepsilon_m^2}{\varepsilon_m^2 - \varepsilon_d^2}exp(-\alpha_0 t_{cav})} \tag{3}$$

and

$$\alpha_0 = \sqrt{\beta_{spp}^2 - \varepsilon_d k_0^2} = \frac{k_0\varepsilon_d}{\sqrt{-\varepsilon_m - \varepsilon_d}} \tag{4}$$

The value of β_{spp} is calculated as:

$$\beta_{spp} = k_0\sqrt{\frac{\varepsilon_m\varepsilon_d}{\varepsilon_m + \varepsilon_d}} \tag{5}$$
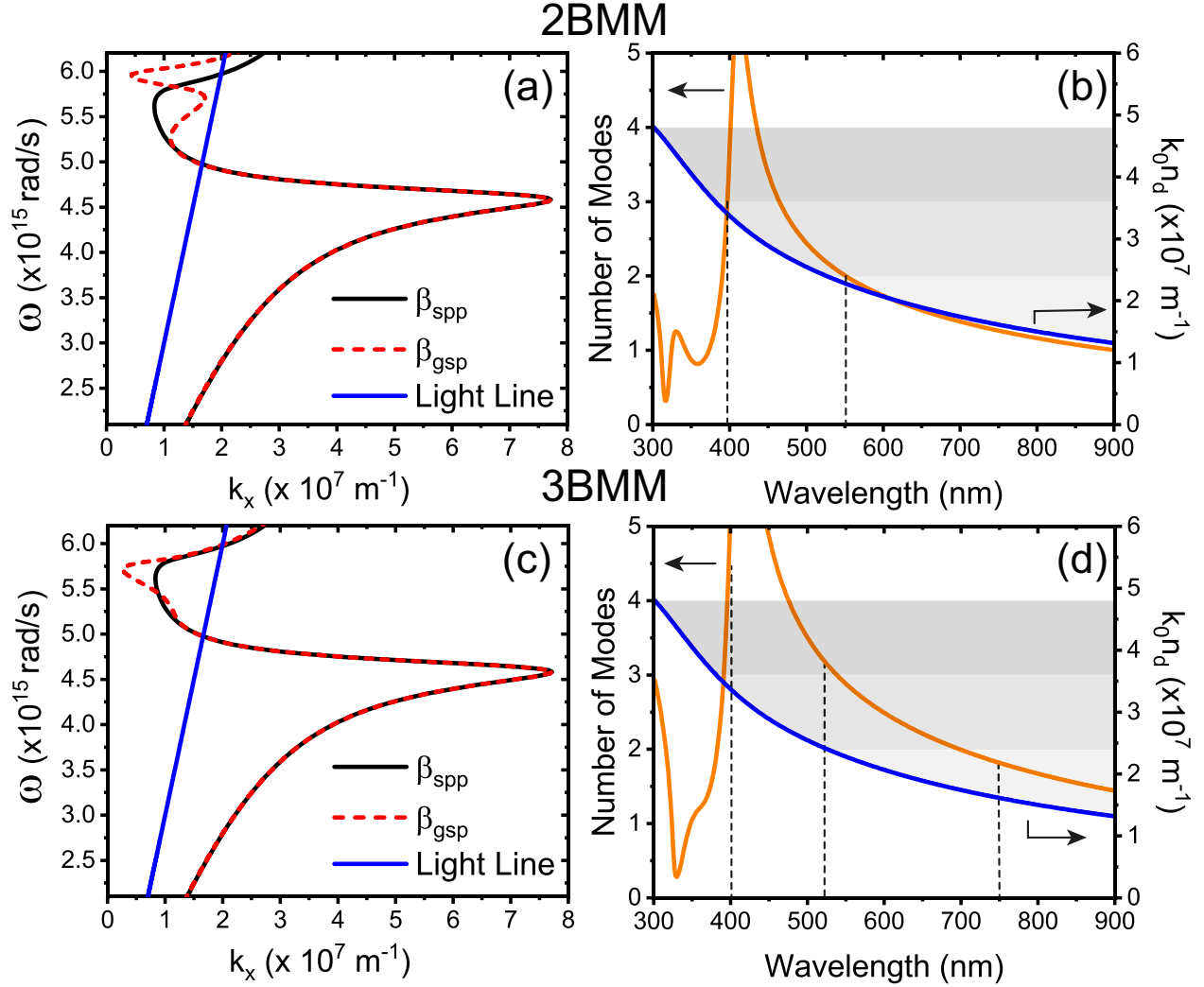
Figure S2: Plots of the dispersion relations of the 2BMM (a) and the 3BMM (c). Modal analysis for the two systems (orange curves), with the permitted region delimited by the dielectric light line (blue curve) (b and d).

In Figures S2a and S2c the dispersion relations of the 2BMM and the 3BMM are reported, respectively. The DRs curves represent the behavior of the angular frequency ω as a function of k_x. By considering a general Fabry-Perot condition, the modes allowed by each cavity are evaluated by using the equation: $\beta t_{cav} = m\pi - \phi$.

In case of a nano-cavity[6], the relation becomes $\beta_{gsp} t_{cav} = m\pi - \phi$, allowing to evaluate the modes in a very simple way. Figures S2b (2BMM) and S2d (3BMM) depict the mode analysis of the two systems, showing also the permitted regions due to the dielectric light line ($k_0 n_d$, blue lines).
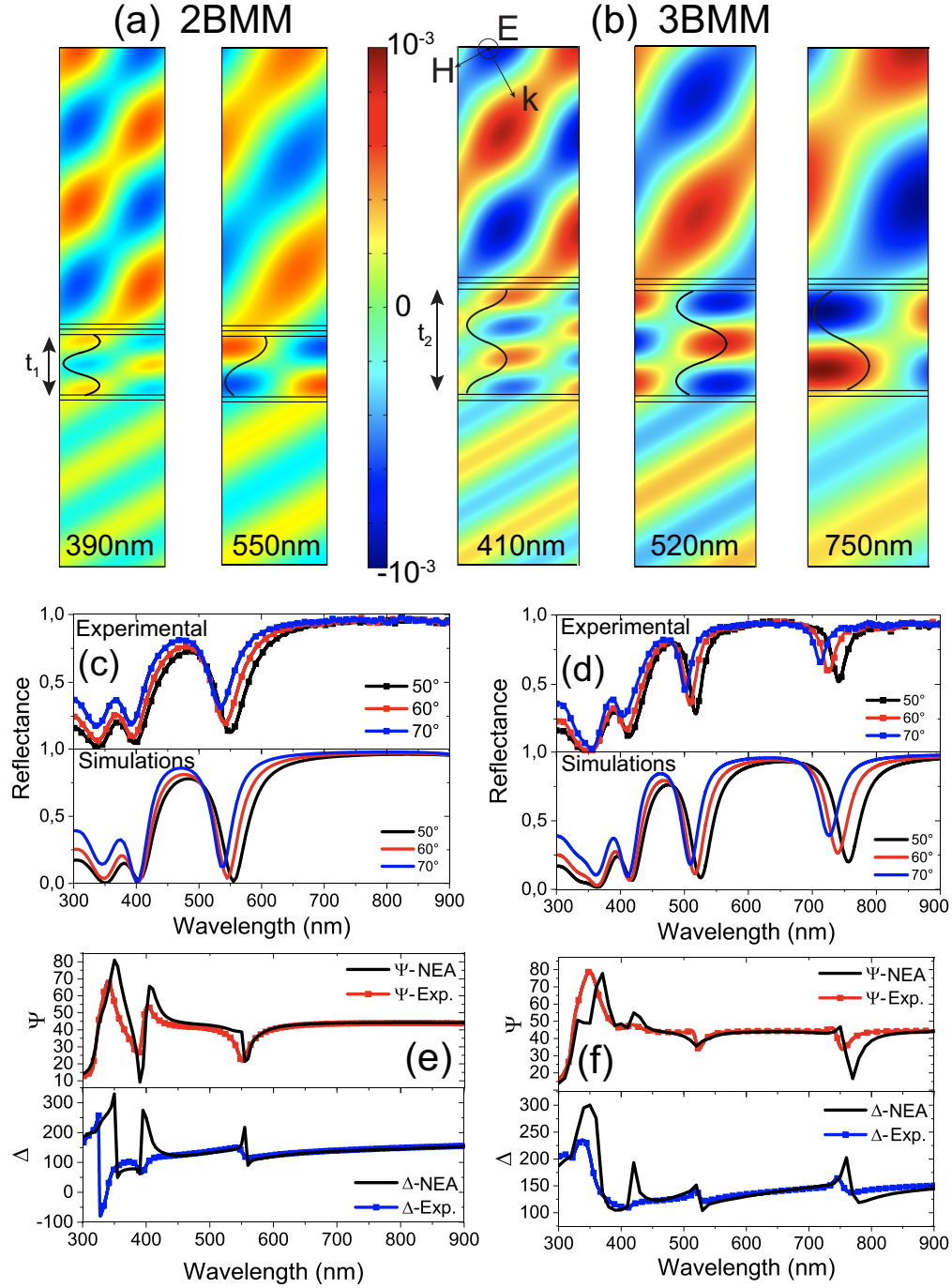
5

Figure S3: Electric field maps (a) for the 2BMM at λ=390nm and λ=550nm, (b) for the 3BMM at λ=410nm, λ=520nm and λ=750nm. Comparison between experimental and the numerical reflectances R_s for the two (c) and three bands metamaterials (d). Ψ and Δ curves are also shown for both systems (e-f).

In figures S3a and S3b the modes related to the 2BMM and 3BMM for TE polarization are depicted as black lines. As evidenced by the field maps, the two structures work as gap cavities for

both polarizations. Figures S3c and S3d show the reflectance curves for s-pol.

The main ellipsometric angles Ψ and Δ are also reported in Figs. S3e and S3f for the two analyzed cases. The experimental and numerical curves of Ψ and Δ are in a very good agreement for the 2BMM, while in the 3BMM case the overlap is not extremely good. This is probably due to a collapse of the thick ITO slab on the thin Ag layer.

The presented COMSOL tool offers also the possibility to evaluate, in a simple way, how the working wavelength can be tuned by acting on the cavity thickness, t_{cav}. Indeed, by varying the thickness from 218 to 242nm, we can move the reflectance dip of about 40nm, passing from 535 to 575nm. In Fig. S4a, it is reported how the reflectance dip redshifts as a function of an increasing thickness value; in Figure S4b the linear trend of the working wavelength as a function of the cavity thickness is shown.
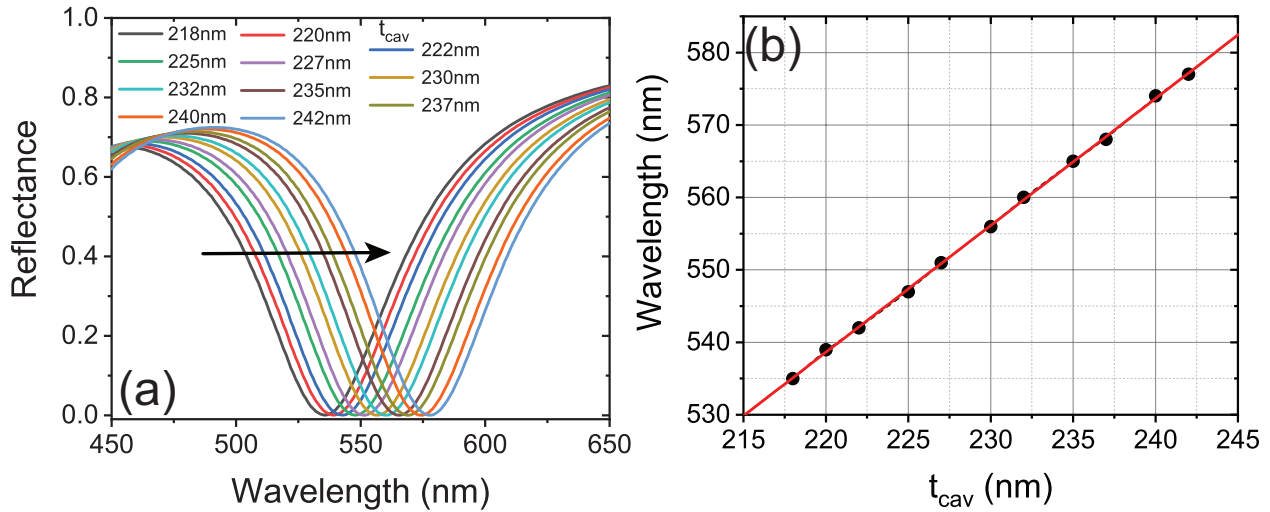

Figure S4: (a) The reflectance dip variation, in terms of position (wavelength), as a function of the cavity thickness t_{cav}, (b) the linear trend between the working wavelength and the cavity thickness (t_{cav}).

In Fig. S5 there is an analysis of the Brewster angle behavior for the 3BMM system and for both incident polarizations. We set the incident wavelength at 750nm and the code allowed to calculate the reflectance profiles by varying the incident angle θ_i. The best value is achieved for p-pol at $\theta_i = 60°$.
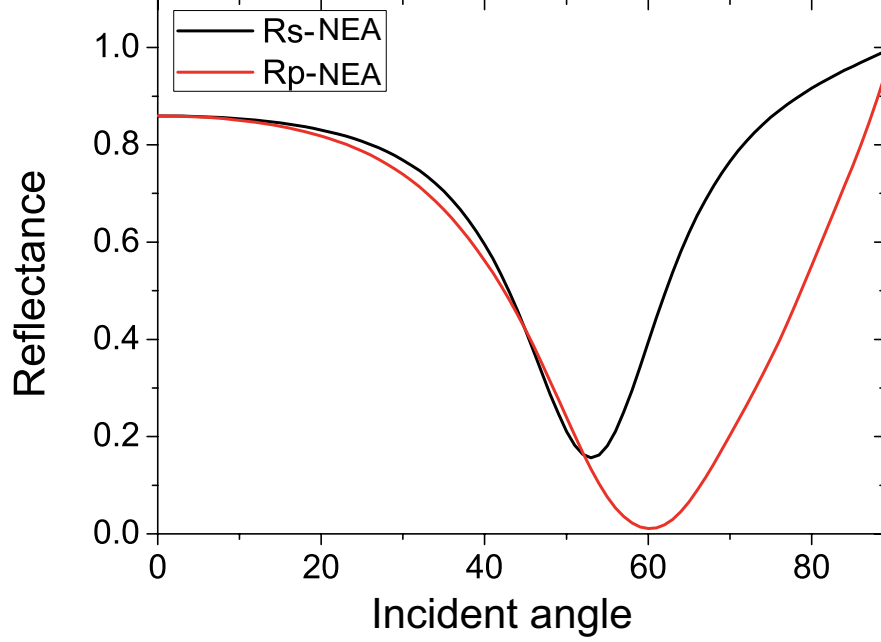
Figure S5: Brewster angle calculated for the 3BMM for both polarizations at λ=750nm.

Comparison tables

Below we report a comparison analysis between two of the four considered cases. In particular, HMM and 2BMM systems have been compared by reporting in two tables the values of reflectance (s- and p- polarizations), transmittance and ellipsometric angles Ψ and Δ, evaluated for six wavelengths from experiments and numerical simulations. As it is evident from the reported data, the comparison highlights that the maximum mismatch between experiments and simulations is of about 7% only in the case of Δ curve for the HMM sample. In all the rest cases this value decreases in average to 2-3%.

Table 1: Comparison between the experimental and the numerical results for the HMM system.

λ (nm)	R_p-EXP	R_p-NEA	R_s-EXP	R_s-NEA	T-EXP	T-NEA	Ψ-EXP (deg)	Ψ-NEA (deg)	Δ-EXP (deg)	Δ-NEA (deg)
300	0.02468	0.01819	0.21684	0.20681	0.00969	0.0108	16.12225	16.51894	176.40642	179.25165
400	0.26989	0.16847	0.13197	0.21046	0.08142	0.22293	51.80153	51.34974	125.90348	175.08376
500	0.82789	0.85623	0.88073	0.88206	0.00488	0.00319	44.06324	44.57705	125.6463	122.7067
600	0.91535	0.92247	0.95269	0.95346	9.4685E-4	8.45813E-4	44.26536	44.52667	136.58073	131.21606
700	0.92753	0.94521	0.96965	0.97096	5.23262E-4	5.43228E-4	44.37718	44.61463	144.10393	140.29522
900	0.9702	0.95832	0.97354	0.98009	7.47689E-4	5.59022E-4	44.50179	44.68209	151.88045	149.17865

Table 2: Comparison between the experimental and the numerical results for the 2BMM system.

λ (nm)	R_p-EXP	R_p-NEA	R_s-EXP	R_s-NEA	T-EXP	T-NEA	Ψ-EXP (deg)	Ψ-NEA (deg)	Δ-EXP (deg)	Δ-NEA (deg)
300	0.16221	0.17137	0.01677	0.10716	0.00572	0.00639	12.75794	14.03969	167.76376	186.24148
400	0.05537	0.03911	0.04418	0.05259	0.41484	0.47891	53.2144	49.22563	249.68987	250.46633
500	0.701	0.75371	0.50593	0.64041	0.2134	0.20178	40.64081	42.669	137.15129	132.23443
600	0.70958	0.71764	0.51731	0.53821	0.4292	0.43295	40.44378	40.89272	124.86029	119.43651
700	0.93015	0.93644	0.8505	0.87026	0.05455	0.0227	43.58876	43.95034	140.22618	137.71113
800	0.96467	0.95986	0.91719	0.90937	0.03024	0.01601	43.9579	44.22595	148.89662	145.3251

References

1. Refki, S.; Hayashi, S.; Rahmouni, A.; Nesterenko, D. V.; Sekkat, Z. Anticrossing behavior of surface plasmon polariton dispersions in metal-insulator-metal structures. *Plasmonics* **2016**, *11*, 433–440.

2. Kuttge, M.; Cai, W.; de Abajo, F. J. G.; Polman, A. Dispersion of metal-insulator-metal plasmon polaritons probed by cathodoluminescence imaging spectroscopy. *Physical Review B* **2009**, *80*, 033409.

3. Bozhevolnyi, S. I. Effective-index modeling of channel plasmon polaritons. *Optics express* **2006**, *14*, 9467–9476.

4. Bozhevolnyi, S.; Volkov, V.; Devaux, E.; Laluet, J.-Y.; Ebbesen, T. Channelling surface plasmons. *Applied Physics A* **2007**, *89*, 225–231.

5. Smith, C. L.; Stenger, N.; Kristensen, A.; Mortensen, N. A.; Bozhevolnyi, S. I. Gap and ed plasmons in tapered grooves: a review. *Nanoscale* **2015**, *7*, 9355–9386.

6. Sorger, V. J.; Oulton, R. F.; Yao, J.; Bartal, G.; Zhang, X. Plasmonic fabry-pérot nanocavity. *Nano letters* **2009**, *9*, 3489–3493.